Ion Atmosphere of Wormlike Micelles Profiled by Contrast Variation Small-Angle Neutron Scattering

Guan-Rong Huang,[*,†] *Christopher N. Lam,*[†] *Kunlun Hong,*[‡] *Yangyang Wang,*[‡] *Yuya Shinohara,*[§] *Changwoo Do,*[†] *and Wei-Ren Chen*[*,†]

[†]Neutron Scattering Division, Oak Ridge National Laboratory, Oak Ridge, Tennessee 37831, United States

[‡]Center for Nanophase Materials Sciences, Oak Ridge National Laboratory, Oak Ridge, Tennessee 37831, United States

[§]Materials Science and Technology Division, Oak Ridge National Laboratory, Oak Ridge, Tennessee 37831, United States

ABSTRACT: Structural studies of wormlike micelles have so far mostly focused on the conformational properties of surfactant aggregates. The diffuse ionic atmosphere, which has profound influence on various micellization phenomena such as thermodynamic stability and structural polymorphism, remains largely unexplored experimentally. In this report a strategy of contrast variation small-angle neutron scattering for this crucial structural study is outlined. Underlined by a general criterion established for unbiasedly identifying the length scale relevant to charge association from the spectral evolution, our analytical framework can provide a quantitative description of counterion distribution in a mathematically tractable manner. Our method can be conveniently extended to facilitate structural studies of complex multi-component systems using contrast-variation neutron scattering.

Electrostatically charged wormlike micelles can be formed via spontaneous self-assembly of amphiphilic molecules in aqueous solutions driven by the hydrophobic effect.[1-2] Because of their various applications,[3-7] wormlike micelles have been extensively studied in the past several decades. Nevertheless, the complexity of the threadlike conformation and long-ranged Coulomb interactions make it challenging to theoretically investigate the microstructures of this important class of material.

Generally speaking, wormlike micelles are complex electrolyte solutions consisting of larger aggregated amphiphilic surfactant molecules and other smaller ions and solvent molecules, with the aggregation size in the range of a few hundred nanometers to several microns. The fundamental influence of electrostatic interactions on the thermodynamic and rheological properties of wormlike micelles is widely appreciated.[8] For example, the structural configuration and stability in solutions are consequences of the screened Coulomb repulsions, which originates from the interaction between electrolyte ions and oppositely charged headgroups of surfactants. Therefore, understanding how the small counterions distribute around the micellar surface is of fundamental importance and technological relevance.[9]

Extensive computational results have identified important ingredients in developing a microscopic description of ionic environment around charged wormlike aggregates:[10-16] The local ion density profile, which gives rise to the screening of repulsive electrostatic interaction, is found to be correlated with the bulk salt concentration and charge density of micellar aggregates. Nevertheless, related experimental studies which directly probe the diffusive ion atmosphere at the relevant length scale are scarce so far. Prominent among the array of the available experimental tools with sufficient spatial resolution are scattering techniques. However, the spatial information of self-assembled nanostructures formed by surfactant molecules, cations and anions, and solvent molecules is concealed in the measured coherent scattering and requires carefully data interpretation. To address the issue properly, one must decompose the contribution of coherent scattering into each constituent of wormlike micelles so as to determine their real-space distribution accordingly. Small angle neutron scattering (SANS) has been demonstrated to be one of the most effective experimental tools for this purpose. Through isotopic labeling, one can increase, annul, or create scattering contrast between different constituents of the sample without altering their spatial distributions, which greatly facilitates the structural reconstruction from spectral analysis. Note that anomalous small angle X-ray scattering also has been used to investigate the counterion distribution in soft matter solution based on the known energy dispersion of targeting counterions.[17] For example, the Sr^{2+} counterion distribution around polyacrylate chains.[17-19] However, for macromolecules with hydrogen and light elements neutrons are more suitable for extracting such distribution.

Using this so-called contrast variation SANS technique,[20-21] in this report we provide a microscopic description of diffuse ion atmosphere in a widely studied charged wormlike micellar system consisting of hexadecyltrimethylammonium bromide (CTAB) and sodium salicylate (NaSal) in aqueous solutions. By adjusting the hydrogen isotope (H/D) ratio of water, the spatial distribution of protonated salicylate anions around the surface of micelles of deuterated CTAB (d-CTAB) surfactants is quantitatively determined based on an approach which circumvents the limitation imposed by the current mean-field framework.

d-CTAB (99.0%) and protonated NaSal (h-NaSal) (99.5%) were purchased respectively from MilliporeSigma and Cambridge Isotope Laboratories, Inc and used without further purification in this study. Deuterium oxide (D_2O, 99.9% purity) was obtained from Cambridge Isotope Laboratories, Inc. Samples with surfactant concentration of 10 mM were prepared at salt-to-surfactant (Cs/Cd) molar ratio of 50. Samples were prepared by weighing the appropriate mass of surfactant and salt and adding the necessary volume of water at five different levels of

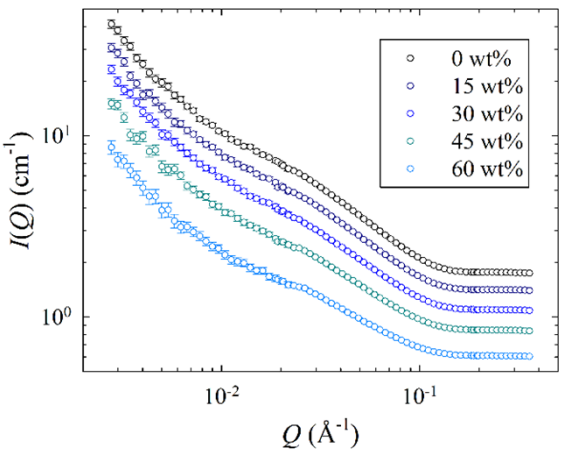

Figure 1. The SANS absolute intensity $I(Q)$ of d-CTAB/h-NaSal solutions with different ratios of H_2O to D_2O. As expected, the absolute intensity of $I(Q)$ is seen to decrease steadily upon increasing the weight fraction of H_2O from 0 wt% to 60 wt%.

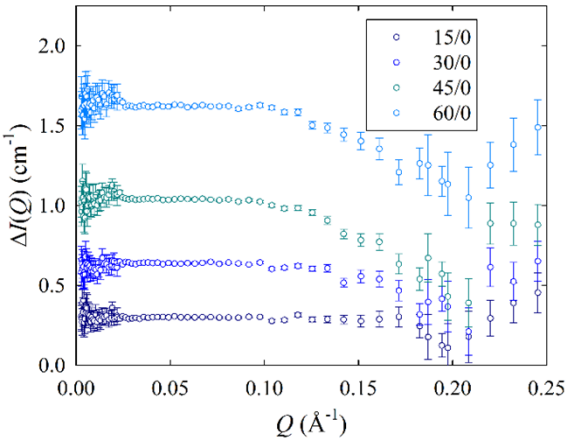

Figure 2. $\Delta I(Q)$ obtained from substituting $I(Q)$ presented in Fig. 1 into Eqn. (2). The $I(Q)$ obtained from the solvent of 100% D_2O is used as the reference point. A steady decrease in the intensity is observed in the range of 0.1 Å$^{-1} < Q < 0.2$ Å^{-1}. $\Delta I(Q)$ remains invariant when $Q < 0.1$ Å^{-1}.

scattering contrast (weight fraction of H_2O/D_2O = 0/100, 15/85, 30/70, 45/55, and 60/40) to achieve the desired concentrations. Samples were mixed for two days and equilibrated for at least one day prior to the experiment. SANS measurements were performed at the Extended Q-Range Small-Angle Neutron Scattering Diffractometer (EQ-SANS) at the Spallation Neutron Source (SNS) of the Oak Ridge National Laboratory (ORNL). The probed Q-range is from 0.003 to 0.4 Å^{-1}. The samples were accommodated in Hellma cells with a path length of 2 mm. During the measurement the temperature range was varied from 5 °C to 45 °C. The measured signal was corrected for detector background, sensitivity, and empty cell scattering, and were normalized by standard procedure of EQ-SANS in order to obtain absolute intensity.

It is worth discussing the mathematical foundation of contrast variation SANS before presenting our experimental result. Discussion within the implementation of this scattering protocol often takes place at two levels. The first one is related to the condition of feasibility: For a system consisting of n principal components characterized by different scattering length densities (SLDs), its SANS coherent scattering cross section $I(Q)$ in the reciprocal Q space can be expressed as[20-21]

$$I(Q) = \sum_{i=1}^{n} n_i v_i^2 \Delta\rho_i^2 S_{ii}(Q) + \sum_{i=1}^{n}\sum_{j\neq i}^{n} \sqrt{n_i n_j} v_i v_j \Delta\rho_i \Delta\rho_j S_{ij}(Q)\,, \quad (1)$$

where n_i and v_i are the number density and volume of component i which are both independent of contrast, $\Delta\rho_i \equiv \rho_i - \rho_s$ represents the excess SLD of component i with respect to the SLD of solvent ρ_s. $S_{ii}(Q)$ is the coherent scattering contribution of component i, and $S_{ij}(Q)$ is the cross coherent scattering contribution originating from the interference of scattered waves of components i and j. Each $\Delta\rho$ varies according to different H/D ratio and in turn results in the change in $I(Q)$. In principle, $S_{ii}(Q)$ and $S_{ij}(Q)$ can be determined from the $I(Q)$ at different scattering contrasts by standard matrix operation. The second one is concerned with the quantitative accuracy of extracted spatial correlations. While it is conceptually straightforward, as indicated by Eqn. (1), that the scattering contribution of each constituent and the cross terms can be uniquely separated assuming the range of D/H ratio is sufficiently explored, determining each partial coherent scattering intensity quantitatively is not trivial.

As the starting point to extract $S_{ii}(Q)$ and $S_{ij}(Q)$ based on the existing protocols, each relevant $\Delta\rho_i$ is required *a priori*. However, how to properly determine their exact values as inputs in Eqn. (1) remains to be a subject of debate. Secondly, the concept of SLD, according to its definition, is only valid in the mean-field limit. It can be intuitively appreciated that for each constituent there exists a certain spatial threshold below which its density becomes ill-defined due to the fussiness of molecular boundary. The value of $\Delta\rho$ therefore is not expected to remain constant within the entire Q range where coherent scattering is observed. As a result, the relevant Q range which conceals the critical information of cross correlation often cannot be straightforwardly identified. Figure 1 presents examples of SANS scattering cross sections collected from aqueous solutions of d-CTAB/h-NaSal. Except for the monotonic decrease of $I(Q)$ with the change of scattering contrast, no clearly discernible features can be extracted to identify the Q range relevant to the association of salicylate anions around the oppositely charged CTAB aggregates. Without this knowledge, it is our conclusion that unique determination of partial and cross coherent intensities based on the matrix operation is inevitably hampered.

Generally, the feature of scattering intensity would be discerned easily by their logarithmic values without incoherent

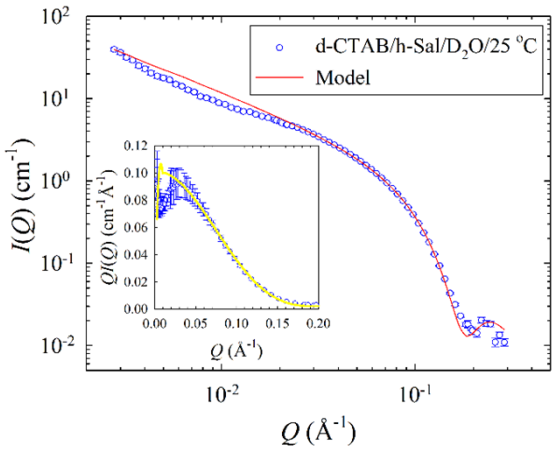

Figure 3. An example of $I(Q)$ without incoherent background (blue symbols) and its corresponding model fitting curve (red curve) predicted by cylindrical macroions with surrounding counterion atmosphere in the Supporting Information. The theoretical description is seen to deviate from the experimental data when $Q < 0.03$ Å^{-1}. The bending rod plot and a regression curve based on the non-interacting wormlike chain model (yellow curve)[19]. Quantitative disagreement is observed when $Q < 0.03$ Å^{-1}. Note that our model fitting at different contrasts also gave the same conclusion.

background. To characterize the difference between scattering curves with different contrasts, we can further subtract them by a reference value. Namely, it can be written as

$$\Delta I(Q) \equiv |\ln I_2(Q) - \ln I_i(Q)|\,, \quad (2)$$

where $I_i(Q)$ is the scattering intensity in solution i and $\ln I_2(Q)$ is the reference value. Obviously, Eqn. (2) will be roughly a constant if the scattering contribution from cations and anions is negligible. Because in this fashion $\Delta I(Q)$ calculated by Eqns. (1) and (2) would be only related to its solution contrast. The results of Eqn. (2) calculated from Fig. 1 are shown in Fig. 2 with the $\ln I_2(Q)$ in 0 wt% H_2O solution. However, when $Q > 0.1$ Å^{-1} there are non-trivial downturns in the curves in Fig. 2. This suggests that within this length scale the scattering contribution cannot be from macroions solely. To characterize the ion atmosphere distribution from Fig. 2, in this report we propose a feasible mathematical protocol to facilitate the data analysis. Without the presence of inter-micellar interaction, $I(Q)$ of our system can be expressed as

$$I(Q) = \left[\sqrt{n_m}\Delta\rho_m v_m F_m(Q) + \sqrt{n_c}\Delta\rho_c v_c F_c(Q)\right]^2 = A[F_m(Q) + xF_c(Q)]^2, \quad (3)$$

where m and c are subscripts used to represent CTAB and salicylate respectively. $A = n_m\,\Delta\rho_m^2 v_m^2$, and $x = \sqrt{\frac{n_c}{n_m}}\frac{\Delta\rho_c}{\Delta\rho_m}\frac{v_c}{v_m}$. $F(Q)$ is the scattering amplitude. Through Eqn. (3), it is straightforward to show that the experimentally measured scattering intensity can be expressed as

$$I(Q) = A\left[P_m(Q) + 2xP_{cross}(Q) + x^2P_c(Q)\right], \quad (4)$$

where $P_m(Q)$, $P_c(Q)$, and $P_{cross}(Q)$ represent the scattering functions of CTAB, salicylate anions and their cross correlation, respectively. As are often the cases of macroions and counterions, x would be much smaller than one because of their disproportionate size difference. We can legitimately expand $\ln I(Q)$ up to the order of x^2 to check the coherent scattering contributed by counterions from the following equation:

$$\ln I(Q) \approx \ln A + \ln P_m(Q) + 2x\frac{P_{cross}(Q)}{P_m(Q)} - x^2\frac{P_c(Q)}{P_m(Q)}, \quad (5)$$

Since $P_m(Q)$, $P_{cross}(Q)$, and $P_c(Q)$ are all independent of SLD, Eqn. (2) can be approximated as the following expression:

$$\Delta I(Q) = (x_1 - x_2)\left[2\frac{P_{cross}(Q)}{P_m(Q)} - (x_1 + x_2)\frac{P_c(Q)}{P_m(Q)}\right] + \ln A_1 - \ln A_2\,. \quad (6)$$

Judging from the definition of A, the value of $\ln A_1 - \ln A_2$ varies upon changing the D/H ratio of solvent but is independent of Q. The Q dependence of $\Delta I(Q)$ is determined by $\frac{P_{cross}(Q)}{P_m(Q)}$ and $\frac{P_c(Q)}{P_m(Q)}$ presenting in the square bracket which are independent from n_m, n_c, $\Delta\rho_m$, $\Delta\rho_c$, v_m and v_c. Since the pre-factor $x_1 - x_2$ is a function of $\Delta\rho_c$, if there is no scattering contribution from salicylate anions within the examined Q range, $\Delta I(Q)$ is expected to be a Q-independent constant value. Therefore Eqn. (6) presents a convenient yet mathematically rigorous tool to identify the Q range relevant to counterion association in this study, as long as the scattering contribution from macroions is dominant. As shown in Fig. 2, the Q range relevant to the diffuse salicylate atmosphere, c.a. 0.1 Å$^{-1} < Q < 0.2$ Å^{-1}, is clearly indicated by this implementation without having to specifying the numerical values $\Delta\rho_c$ and $\Delta\rho_m$ in advance. Therefore, the identified Q range is free from any artificial interference.

Guided by Fig. 2, we now can readily proceed to quantitative data analysis. The fact that $\Delta I(Q)$ essentially remains constant when $Q < 0.1$ Å^{-1} suggests that the information of $I(Q)$ in this Q range is irrelevant for determining the counterion association. Therefore, the focus of our scattering function development is placed on providing a quantitative description of $I(Q)$ given in Fig. 1 in the range of $Q > 0.1$ Å^{-1}. Within this microscopic length scale, our charged micellar system is schematically considered as a collection of rigid cylinders dressed by ionic cloud and immersed in structureless background water. We assume that counterions distribute uniformly along the direction of cylinder axis and have the same dimension as that of macroions. Meanwhile, in the direction of cylinder cross-section counterions distribution decay monotonically and mostly reside outside the surface of macroions. Namely, counterions only exist beyond the radius of macroions, R. Based on this conceptual picture, we developed $P_m(Q)$, $P_c(Q)$, and $P_{cross}(Q)$ accordingly. Their analytical expressions and details of data analysis are given in the Supporting Information. We give a comparison of the measured $I(Q)$ and the corresponding model fitting curve in Fig. 3. A satisfactory quantitative agreement is observed when

$Q > 0.03$ Å^{-1}, suggesting that the spatial distribution of salicylate anions around the cationic surfactant aggregates can be reliably extracted based on our developed scattering functions. It is instructive to discuss the disagreement between the theoretical and experimental scattering functions observed in the low Q regime: As indicated by the bending rod plot given in the inset, the global structure of charged CTAB aggregates cannot be described by the wormlike chain conformation.[22] It is our conjecture that under this ionic condition, certain degree of branching could have developed.[23] As indicted by the combined USANS-SANS coherent scattering cross section given in the Supporting Information, no extended-range structure is observed judging from the statistics of USANS signal. Nevertheless, the main scattering features of the local cylindrical structure of these charged micellar systems reflected in the spatial range probed by SANS can still be captured by our current model.

In developing the functional form of $P_c(Q)$, the distribution of salicylate anions around the surface of cationic CTAB aggregates is assumed to follow the feature of Poisson-Boltzmann distribution,[24-25] namely its number density along the radial direction of cylinder cross-section is proportional to an exponential decay with a characteristic length or so-called Debye length λ_D from the micellar surface towards the surrounding solvent. From the structural parameters optimized in the regression process, the spatial distribution of salicylate can be determined based on this framework. From the concentration profiles of salicylate anions given in Fig. 4, we have found that the ionic environment around the charged CTAB aggregates declines monotonically within the temperature variation of 5 °C to 45 °C. However, the characteristic length of these distributions is insensitive to this temperature range. As shown in the inset, no quantitatively distinct dependence of λ_D on temperature is found. In general, the Debye length has the following expression

$$\lambda_D = \sqrt{\frac{\varepsilon k_B T}{\sum_j n_j^0 q_j^2}}, (7)$$

where ε is the dielectric constant, k_B is the Boltzmann constant, T is the absolute constant, q_j is the charge of jth ion, and n_j^0 is the concentration of jth ion. Within this probed temperature range, λ_D essentially remains around 5 Å. In electrolyte solution, λ_D would be proportional to the square root of the ratio of absolute temperature to ion strength as indicated in Eqn. (7).[26-28] Given that our NaSal concentration is fixed, λ_D would be proportional to the square root of absolute temperature. Within this temperature range, we can expect no appreciable changes on λ_D values. It is noted that Shukla and Rehage have reported $\lambda_D = 8\,nm$ in the CTAB/NaSal solution with Cs/Cd = 0.33 and 30 °C based on their results of light scattering.[29] In our CTAB/NaSal solution with Cs/Cd = 50, the extrapolation estimation by Cs/Cd ratio would give $8\,nm \times \sqrt{0.33/50} \approx 6.5$ Å, which is consistent with our extracted values. Around this concentration, the counterions are condensed around the periphery of macroions. Therefore, the length scale would not be as large as that of Ref. [29].

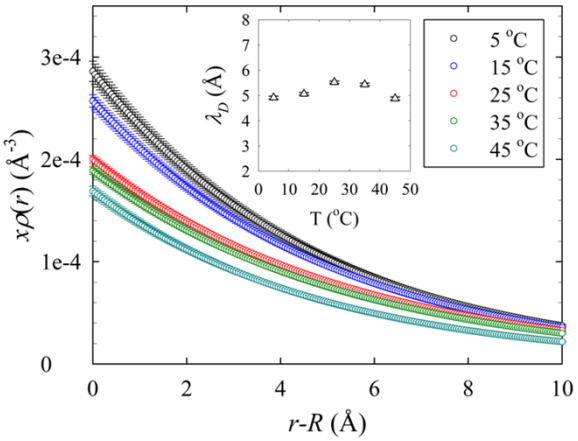

Figure 4. The concentration profiles of salicylate anions around the surface of cationic CTAB aggregates obtained at different temperatures with 0 wt% H_2O. R is the radius of cylindrical cross-section. The details of model fitting are in the SI. The inset gives the evolution of Debye length as a function of temperature.

In summary, we have quantitatively revealed the ionic environment in a commonly studied wormlike micellar system using the technique of contrast variation SANS. By observing the difference between scattering intensities with different contrasts, we showed that the scattering signal from counterion is no longer negligible. Complemented by a prognostic criterion which indicates the spatial range relevant to counterion association, the spatial range of diffuse counterion around the surface of cationic surfactant aggregates can be determined precisely. We further construct the analytical scattering functions of CTAB and counterions to analyze the ion atmosphere distribution along the radial direction. In comparison to the existing approaches, our criterion does not require pre-determined scattering characteristics of structural constituents as inputs to obtain the relevant length scale of isotopically labeled species. Therefore, it presents a practical solution to avoid the potential issue of biased interpretation of experimental data with scattering model fitting. Moreover, the framework developed in this study not only is able to quantify the ion environment of polyelectrolyte self-assembly systems, as demonstrated in the Supporting Information, it can also be extended to facilitate contrast vitiation SANS investigation of complex multicomponent systems commonly encountered in the structural study of soft matter.

ASSOCIATED CONTENT

Supporting Information.

1. Derivation of scattering function of cylindrical CTAB aggregates.
2. Derivation of scattering function of diffuse salicylate anions around the surface of cationic CTAB aggregates.
3. Derivation of cross correlation function of CTAB aggregates and salicylate anions.

4. Generalization of the prognostic criterion.
5. Combined USANS-SANS coherent scattering cross section of d-CTAB/h-NaSal solutions.

AUTHOR INFORMATION

Corresponding Author

*E-mail: huangrn@ornl.gov; chenw@ornl.gov

ACKNOWLEDGMENT

This research was performed at the Spallation Neutron Source (SNS) and the Center for Nanophase Materials Sciences (CNMS), which are the U.S. Department of Energy Office of Science User Facilities operated by Oak Ridge National Laboratory. YW is supported by the U.S. Department of Energy, Office of Science, Office of Basic Energy Sciences, Early Career Research Program Award KC0402010, under Contract DE-AC05-00OR22725. YS is supported by the U.S. Department of Energy, Office of Science, Office of Basic Energy Sciences, Materials and Science and Engineering Division. We gratefully appreciate the EQSANS and USANS beamtime from SNS.

REFERENCES

(1) Clausen, T.M.; Vinson, P. K.; Minter, J. R.; Davis, H. T.; Talmon, Y.; Miller, W. G. Viscoelastic Micellar Solutions: Microscopy and Rheology. *J. Phys. Chem.* **1992,** *96,* 474–484.

(2) Lin, Z.; Scriven, L. E.; Davis, H. T. Cryogenic Electron Microscopy of Rodlike or Wormlike Micelles in Aqueous Solutions of Nonionic Surfactant Hexaethylene Glycol Monohexadecyl Ether. *Langmuir* **1992,** *8,* 2200–2205.

(3) Chase, B.; Chmilowski, W.; Marcinew, R.; Mitchell, C.; Dang, Y.; Krauss, K.; Nelson, E.; Lantz, T.; Parham, C.; Plummer, J. Clear Fracturing Fluids for Increased Well Productivity. *Oilf. Rev.* **1997,** *9,* 20–33.

(4) Rose, G. D.; Foster, K. L. Drag Reduction and Rheological Properties of Cationic Viscoelastic Surfactant Formulations. *J. Nonnewton. Fluid Mech.* **1989,** *31,* 59–85.

(5) Zhang, J.; Wang, L. Q.; Wang, H.; Tu, K. Micellization Phenomena of Amphiphilic Block Copolymers Based on Methoxy Poly(ethylene glycol) and Either Crystalline or Amorphous Poly(caprolactone-b-lactide). *Biomacromolecules* **2006,** *7,* 2492–2500.

(6) Dong, C. M.; Chaikof, E. L. Self-Assembled Nanostructures of a Biomimetic Glycopolymer–Polypeptide Triblock Copolymer. *Colloid Polym. Sci.* **2005,** *283,* 1366–1370.

(7) Dalhaimer, P.; Engler, A. J.; Parthasarathy, R.; Discher, D. E.; Targeted Worm Micelles. *Biomacromolecules* **2004,** *5,* 1714–1719.

(8) For example, see Dreiss, C. A. Wormlike Micelles: Where do We Stand? Recent Developments, Linear Rheology and Scattering Techniques. Soft Matter **2007,** *3,* 956–970 and references therein.

(9) Berret, J.-F. in *Molecular Gels: Materials with Self-Assembled Fibrillar Networks*, Edited by Weiss, R. G.; Terech, P. Springer: Dordrecht, 2006.

(10) Yakovlev, D. S.; Boek, E. S. Molecular Dynamics Simulations of Mixed Cationic/Anionic Wormlike Micelles. *Langmuir* **2007,** *23,* 6588-6597.

(11) Padding, J. T.; Boek, E. S.; Briels, W. J. Dynamics and Rheology of Wormlike Micelles Emerging from Particulate Computer Simulations. *J. Chem. Phys.* **2008,** *129,* 074903.

(12) Wang, Z.; Larson, R. G. Molecular Dynamics Simulations of Threadlike Cetyltrimethylammonium Chloride Micelles: Effects of Sodium Chloride and Sodium Salicylate Salts. *J. Phys. Chem. B* **2009,** *113,* 13697–13710.

(13) Kuriabova, T.; Betterton, M. D.; Glaser, M. A. Linear Aggregation and Liquid-Crystalline Order: Comparison of Monte Carlo Simulation and Analytic Theory. *J. Mater. Chem.* **2010,** *20,* 10366–10383.

(14) Wang, Y.; Wallace, J. A.; Koenig, P. H.; Shen, J. K. Molecular Dynamics Simulations of Ionic and Nonionic Surfactant Micelles with a Generalized Born Implicit-Solvent Model. *J. Comput. Chem.* **2011,** *32,* 2348–2358.

(15) Sangwai, A. V.; Sureshkumar, R. Coarse-Grained Molecular Dynamics Simulations of the Sphere to Rod Transition in Surfactant Micelles. *Langmuir* **2011,** *27,* 6628–6638.

(16) Brodskaya, E. N. Computer Simulations of Micellar Systems. *Colloid J.* **2012,** *74,* 154–171.

(17) Stuhrmann, H. B. Resonance scattering in macromolecular structure research. *Adv. Polym. Sci.* **1985**, 67, 123.

(18) Goerigk, G.; Schweins, R.; Huber, K.; Ballauff, M. The distribution of Sr^{2+} counterions around polyacrylate chains analyzed by anomalous small-angle X-ray scattering. *Europhys. Lett.* **2004**, 66, 331-337.

(19) Goerigk, G.; Huber, K.; Schweins, R. Probing the extent of the Sr^{2+} ion condensation to anionic polyacrylate coils: A quantitative anomalous small-angle X-ray scattering study. *J. Chem. Phys.* **2007**, 127, 154908.

(20) Williams, C. E. in *Neutron, X-rays and Light. Scattering: Introduction to An Investigative Tool for Colloidal and Polymeric Systems*, Edited by Lindner, P.; Zemb, Th.; North-Holland: Amsterdam, 1991.

(21) Cotton, J. P., Variations on Contrast in SANS: Determination of Self and Distinct Correlation Functions. Adv. Colloid Interface Sci. **1996,** *69,* 1-29.

(22) Chen, W.-R.; Butler, P. D.; Magid, L. J. Incorporating Intermicellar Interactions in the Fitting of SANS Data from Cationic Wormlike Micelles. *Langmuir* **2006,** *22,* 6539-6548.

(23) Lin, Z. Branched Worm-like Micelles and Their Networks. *Langmuir* **1996,** *12,* 1729-1737.

(24) Schmitz, K. S. *Dynamic Light Scattering by Macromolecules*; Academic Press, Inc.: San Diego, 1990.

(25) Schmitz, K. S. *Macroions in Solution and Colloidal Suspension*; VCH Publishers, Inc.: New York, 1993.

(26) Russel, W. B.; Saville, D. A.; Schowalter W. R. *Colloidal Dispersions,* Cambridge University Press, 1989.

(27) Dukhin, A. S.; Gotez, P. J. *Characterization of liquids, nano- and micro-particulates and porous bodies using Ultrasound*, Elsevier, 2017.

(28) Colloidal systems – Methods for Zeta potential determination- Part 1: Electroacoustic and Electrokinetic phenomena*, International Standard ISO 13099-1*, 2012.

(29) Shukla, A.; Rehage, H. Zeta Potentials and Debye Screening lengths of Aqueous, Viscoelastic Surfactant Solutions (Cetyltrimethylammonium Bromide/Sodium Salicylate System). *Langmuir* **2008**, *24*, 8507–8513.